A self-consistent tight binding model for hydrocarbon systems: application to quantum transport simulation

2004 J. Phys.: Condens. Matter 16 6851

(http://iopscience.iop.org/0953-8984/16/39/018)

INSTITUTE OF PHYSICS PUBLISHING JOURNAL OF PHYSICS: CONDENSED MATTER

J. Phys.: Condens. Matter **16** (2004) 6851–6866 PII: S0953-8984(04)71242-4

A self-consistent tight binding model for hydrocarbon systems: application to quantum transport simulation

D A Areshkin, O A Shenderova, J D Schall, S P Adiga and D W Brenner

Department of Materials Science and Engineering, North Carolina State University, Raleigh, NC 27695-7907, USA

E-mail: denis@alchemy.nrl.navy.mil

Received 30 October 2003, in final form 20 August 2004
Published 17 September 2004
Online at stacks.iop.org/JPhysCM/16/6851
doi:10.1088/0953-8984/16/39/018

Abstract

A self-consistent environment-dependent (SC-ED) tight binding (TB) method for hydrocarbons that was developed for quantum transport simulations is presented. The method builds on a non-self-consistent environment-dependent TB model for carbon (Tang *et al* 1996 *Phys. Rev.* B **53** 979) with parameters added to describe hydrocarbon bonds and to account for self-consistent charge transfer. The SC-EDTB model assumes an orthogonal basis set. Orthogonality is a key element for adapting the SC-EDTB scheme to transport problems because it substantially increases the efficiency of the Newton–Raphson algorithm used to accelerate self-consistency convergence under non-equilibrium conditions. Compared to most existing TB schemes the SC-EDTB scheme is distinctive in two respects. First, self-consistency is added through the exact evaluation of Hartree and linear expansion of exchange integrals. All Hamiltonian elements belonging to the same atom are affected by charge transfer, not just the diagonal elements. The second distinction is the choice of SC-EDTB parameters; they were fitted to Mulliken populations and eigenvalue spectra rather than energies or elastic properties. The former are directly related to the conductivity and potential profile, which are essential for transport simulation. No two-centre repulsive term parametrization was performed. The functionality of the method is exemplified by computing I–V curves, non-equilibrium potential profiles and current density for a resonant tunnelling device.

(Some figures in this article are in colour only in the electronic version)

1. Introduction

Techniques for quantum transport simulation [1–7] are very important for the development of molecular electronics [8]. Many of these techniques are based on a non-equilibrium Green function (NEGF) approach [1, 2], and electronic structure methods (ESM). The majority of reported transport simulations can be divided into two categories according to the ESM being employed. The first category is based on unsophisticated tight-binding (TB) schemes that are computationally efficient but that lack precision [2, 3]. The second category uses well established density functional theory (DFT) codes [1, 5–7] (e.g. Gaussian), which were not created specifically for transport problems, and hence are constrained to small and well behaved systems. Presented in this paper is an ESM that is optimized for use with NEGF algorithms. The choice of ESM is stipulated by the requirements described below.

Transport problems usually involve systems that are partially or completely metallic. A voltage drop in a metal is a purely non-equilibrium effect and, in general, cannot be approximated by an applied external field. A self-consistent NEGF approach must be used to obtain the correct voltage distribution in a metallic system under an external bias. Hence self-consistency is the first requirement for the ESM of our choice.

It is impossible to employ any of the existing $O(N)$ algorithms for evaluating the non-equilibrium density matrix because the energy functional minimization can be used only for the ground state solution. In the NEGF approach the density matrix is computed by contour integration of Green matrices. Each sampling point on the integration contour is obtained through matrix inversion, which is an $O(N^3)$ operation (N is the number of orbitals in the system). Thus, the number of operations required by each self-consistency iteration is $O(N^3)$ times the number of sampling points. Contour integration is parallelizable, though the number of sampling points usually overwhelmingly exceeds the number of processors. $O(N^3)$ scaling imposes a severe restriction on the ESM candidate; if reasonably large systems ($\sim$100–500 atoms) are targeted, the ESM should use a minimal basis set.

Simple charge mixing often does not lead to a converged self-consistent solution, especially in metals. To ensure fast and guaranteed convergence towards self-consistency, special algorithms should be engaged. However, most convergence acceleration algorithms (see [9] and the discussion therein) are based on the correspondence of a self-consistent solution to minimum total energy. Obviously this property cannot be used in non-equilibrium problems. On the other hand, convergence acceleration methods that employ the derivative of the output charge density with respect to input charge density (e.g. Broyden [10] or Newton–Raphson [11]) are still valid and can be applied to non-equilibrium cases. The size M of the derivative matrix A equals the number of unique atomic orbital products contributing to the total electron density. M is the number of $\{\alpha, \beta\}$ pairs ($\alpha \leqslant \beta$) such that for some r

$$\varphi_\alpha(r)\varphi_\beta(r) \neq 0. \tag{1}$$

Possible values of M lie in the interval $\{N, N(N+1)/2\}$. The Broyden method computes the derivative matrix iteratively. The number of iterations required to obtain the precise value of A is M. Thus the total number of operations per sampling point required to achieve self-consistency is $O(MN^3)$. In the Newton–Raphson algorithm the exact value of the matrix A is computed at each iteration. The total cost of computing A using the Newton–Raphson algorithm in conjunction with an NEGF formalism is $O(M^3) + N_{SP}O(M^2)$, where N_{SP} is the number of sampling points on the integration contour. The number of iterations required to achieve self-consistency NI_{SC} usually varies between 5 and 15. The total number of operations for the Newton–Raphson algorithm is $NI_{SC}(N_{SP}(O(N^3) + O(M^2)) + O(M^3))$. If $M \sim N$ the Newton–Raphson algorithm is preferred over the Broyden method. The

smallest possible value of $M = N$ is achieved when condition (1) is satisfied only for $\alpha = \beta$. We term this approximation 'diagonal'. In the diagonal approximation atoms cannot produce dipole moments, and act almost like spherical charges. The next, more advanced degree of precision, which we term 'block-diagonal', is achieved when condition (1) is satisfied only if orbitals α and β belong to the same atom. In this case an atom can create a dipole moment by superposition of s- and p-type atomic orbitals. This property is very important for a correct description of the potential produced by asymmetrical or dangling bonds. Under the minimal basis set assumption every carbon atom has four orbitals. Under the block-diagonal approximation there are ten unique $\{\alpha, \beta\}$ pairs per carbon atom for which condition (1) is satisfied. For systems composed of carbon atoms $M = 2.5N$, and the total workload for evaluating matrix A increases by a factor of $2.5^3 \cong 16$ compared to the diagonal approximation. The total number of operations towards self-consistency is $NI_{\mathrm{SC}}((N_{\mathrm{SP}} + 16)\mathrm{O}(N^3))$. The next degree of precision is achieved when equation (1) is satisfied only if α and β belong either to the same atom or to the nearest neighbours. In a diamond lattice $M = (2.5 + 4 \times 4)N$. The total number of operations required for self-consistency is $NI_{\mathrm{SC}}((N_{\mathrm{SP}} + (18.5)^3)\mathrm{O}(N^3))$. The number of sampling points N_{SP} in the example presented in section 5 gradually increases from 50 to 600 as the solution approaches self-consistency. This number is substantially less than $(18.5)^3 \cong 6332$. Additionally, it becomes problematic to store matrix M even for moderate-size (e.g. 300 atoms) systems.

The block-diagonal approximation seems a reasonable compromise between the quality of the charge density description and the computational workload. We adopt it as an additional constraint for the ESM being constructed. The block-diagonal approximation corresponds to an orthogonal overlap matrix. However, it should be noted that the term 'orthogonal basis set' is not exactly applicable here. If φ_α and φ_β belong to different atoms, the orthogonal basis set requirement means that $\int \varphi_\alpha(r)\varphi_\beta(r)\,\mathrm{d}r = 0$, while the block-diagonal approximation assumes that $\varphi_\alpha(r)\varphi_\beta(r) = 0$ for any r.

Besides self-consistency and performance issues an adequate description of electron potential, energy spectra, and electron density response to applied fields are of high priority for a desired ESM. Special care should be taken to accurately convey energy spectra in the vicinity of the Fermi level because that energy region is the most important for electronic transport. These tasks can be viewed as a constrained optimization problem, where the constrains are a minimal orthogonal basis set and the block-diagonal approximation. Therefore the choice for ESM is limited to either an orthogonal minimal basis set DFT or self-consistent TB.

In 1996 Ho and coworkers introduced a non-self-consistent environment dependent TB (EDTB) scheme for carbon [12]. 'Environment dependent' means that the hopping matrix elements depend not only on the distance between the two atoms on which basis functions are centred, but also on the arrangement of neighbouring atoms. Sometimes it is convenient to view the TB method as a simplified DFT in which the matrix elements rather than the atomic orbitals are specified. From this standpoint the EDTB concept is analogous to a DFT scheme that accounts for three- and four-centre integrals, and with atomic orbitals adjusting to the atomic environment. This concept seems to produce more transferable results than a fixed orthogonal minimal basis set DFT under the block-diagonal restriction. The EDTB scheme, which is briefly discussed in section 2, is the starting point for developing the self-consistent method described in section 3.

The remainder of this paper is organized as follows. Section 4 contains a description of the Newton–Raphson method joined with the NEGF approach. Section 5 describes an application of the self-consistent EDTB scheme to the simulation of current density and I–V curves for a resonant tunnelling device.

In the present paper we are not interested in total energies and atomic forces (e.g. for a molecular dynamics simulation); thus the self-consistent EDTB parametrization does not include these quantities in the fitting scheme.

2. EDTB scheme

The traditional feature of most TB methods is a two-centre Hamiltonian matrix parametrization, which implies the neglect of three- and four-centre integrals as well as nonlinearities of the exchange–correlation potential [13]. This means that the contribution of the molecular potential $V(r)$ to the Hamiltonian matrix element $H_{\alpha\beta}$ is restricted to $\langle\varphi_\alpha|V_i(r)|\varphi_\beta\rangle$, where either atomic orbital φ_α or φ_β belongs to the ith atom producing potential $V_i(r)$. To augment the contributions with index i belonging to atomic sites other than those on which φ_α or φ_β are centred, the original EDTB uses a screening function $S_{\alpha\beta}$ and a scaling function $R_{\alpha\beta}$ that transform the conventional form for two-centre Hamiltonian matrix elements as $H_{\alpha\beta}(r_{\alpha\beta}) \rightarrow H_{\alpha\beta}[R_{\alpha\beta}(r_{\alpha\beta})](1 - S_{\alpha\beta})$. The parameterized functions $S_{\alpha\beta}$ and $R_{\alpha\beta}$ depend on the positions of neighbour atoms, and are designed to account for the influence of atomic environment on two-centre Hamiltonian matrix elements. For example, when no other atoms are in the vicinity of the line connecting φ_α or φ_β, $S_{\alpha\beta}$ is zero. When an extra atom appears between φ_α and φ_β the value of $S_{\alpha\beta}$ increases because the extra atom screens the two-centre interaction, and the contribution to $H_{\alpha\beta}$ then comes primarily from the three-centre integral.

The function $R_{\alpha\beta}$ has four parameters, and $S_{\alpha\beta}$ uses separate sets of four parameters for each type of hopping integral, allowing a good fit to band structures from DFT calculations for six lattice types with atomic coordinations that vary from 2 to 12. Fitting to multiple band structures helps to ensure that the EDTB method is applicable to non-periodic systems with a variety of coordination numbers and is more transferable than conventional TB schemes. For example, an indirect bandgap for diamond versus a direct band gap given by the Xu *et al* parametrization [14] is achieved with the EDTB method.

The EDTB model was not the first attempt to include three-centre integrals in a TB scheme. In 1989 Sankey and Niklewski introduced a parameter-free DF-TB scheme that is essentially a minimal non-orthogonal basis set DFT calculation, but with matrix elements precalculated on a coarse grid [15]. Interpolation between grid points is used to evaluate matrix elements for the given set of distances and angles. Frauenheim and co-workers introduced a similar DF-TB scheme based on two-centre integrals [16].

The main advantage of the DF-TB schemes over other TB approaches is that in principle they do not require parameter fitting. However, the DF-TB models use a fixed atomic orbital basis, while the EDTB method accommodates the 'orbitals' to atomic environments, a potential advantage in terms of the transferability of the scheme for describing electronic states of carbon in different bonding configurations.

3. SC-EDTB scheme

To further expand the transferability and functionality of TB schemes, a number of methods have been implemented that introduce self-consistency into TB electronic states (see [13] for a review). Historically, most of these involved modifications to existing non-self-consistent schemes. For example, Frauenheim *et al* enhanced a two-centre DF-TB approach [16] by adding self-consistent (SC) terms [17] and spin polarization [18] that could be used with an O(N) scaling scheme [19]. Similarly, SC versions of Sankey's multicentre DF-TB scheme [20], as well as Halley and coworker's TB approach [21, 22], have been introduced, with the latter adding spin-polarized terms to study magnetic systems [23].

3.1. Formalism

In this paper an SC modification to the EDTB scheme for carbon is introduced that allows charge transfer and applied fields to be modelled. In this approach, which we term the SC-EDTB method, the Hamiltonian matrix H is composed of two parts, the original EDTB matrix $H0$, and SC corrections ΔH. The latter accounts for charge transfer between constituent atoms, and is supposed to be zero for periodic structures for which the original non-SC EDTB parametrization was made. To be consistent with its initial implementation, the EDTB should be extended to include self-consistency by using a DF-based approach analogous to [16, 21, 24] but for a basis set that is adjustable to different atomic environments. However, we approach the problem in a less efficient, though simpler manner and use an environment independent basis to compute ΔH.

Suppose that the EDTB method was derived as a non-SC DF-TB, i.e. $H0$ matrix elements were obtained from applying a Hamiltonian operator to atomic orbitals $\varphi_\zeta(r)$ rather than from a fitting procedure. In that case for some periodic reference structure, described by Hamiltonian $H0_{\mathrm{ref}}$, we can construct the charge density $\rho_{\mathrm{ref}}(r)$. A small deviation of $\delta\rho(r)$ from $\rho_{\mathrm{ref}}(r)$ changes the matrix elements of $H0_{\mathrm{ref}}$ by

$$\Delta H_{\alpha,\beta} = \int \varphi_\alpha(r)\left[\int \frac{\delta\rho(R)}{|r-R|}\,\mathrm{d}R + \Delta V_{\mathrm{xc}}(r)\right]\varphi_\beta(r)\,\mathrm{d}r. \tag{2}$$

Here ΔV_{xc} is the change in the exchange–correlation potential associated with $\delta\rho(r)$. ΔV_{xc} is approximated by linear expansion of exchange component $V_{\mathrm{ex}} = -\rho^{1/3}(3/\pi)^{1/3}$:

$$\Delta V_{\mathrm{ex}}(r) \approx (\partial V_{\mathrm{ex}}(\rho)/\partial\rho)_{\rho=\rho(r)_{\mathrm{ref}}}\delta\rho(r). \tag{3}$$

If the block-diagonal approximation is assumed, ΔH has a block-diagonal structure with 4×4 and 1×1 blocks corresponding to carbon and hydrogen atoms, respectively.

Equation (2) may be used to add a charge transfer capability, and hence self-consistency, to any TB scheme, not necessarily a DF-based approach. In that case ΔH must be zero for a reference structure fitted by the non-SC TB approach, and atomic orbital parameters are obtained through the fitting procedure. Such an approach is employed to convert the EDTB method into the SC-EDTB method. After orbital parameters are chosen, $\rho_{\mathrm{ref}}(r)$ is defined as

$$\rho_{\mathrm{ref}}(r) = \sum_i \sum_{\{\alpha,\beta\}} D^{\mathrm{ref}}_{i,\{\alpha,\beta\}}\varphi_\alpha(r-R_i)\varphi_\beta(r-R_i). \tag{4}$$

Here α and β belong to the same atom, R_i denotes the coordinates of the ith atom, and $D^{\mathrm{ref}}_{i,\{\alpha,\beta\}}$ is a (non-SC) density matrix corresponding to $H0_{\mathrm{ref}}$. If a minimal sp^3 basis set is used, and the reference structure is a bulk crystal with high symmetry (e.g. diamond, fcc, sc, bcc), the reference density is composed of identical spherically symmetric atomic densities

$$\rho_{\mathrm{ref}}(r) = \sum_i \rho^{\mathrm{atom}}_{\mathrm{ref}}(|r-R_i|), \qquad \text{where } \rho^{\mathrm{atom}}_{\mathrm{ref}}(|r|) = \sum_{\{\alpha,\beta\}} D^{\mathrm{ref}}_{\alpha,\beta}\varphi_\alpha(r)\varphi_\beta(r). \tag{5}$$

If an arbitrary atomic configuration is considered, its density can be represented as

$$\rho(r) = \sum_i \rho^{\mathrm{atom}}_{\mathrm{ref}}(|r-R_i|) + \sum_i \sum_{\{\alpha,\beta\}} (D_{i,\{\alpha,\beta\}} - D^{\mathrm{ref}}_{\alpha,\beta})\varphi_\alpha(r-R_i)\varphi_\beta(r-R_i). \tag{6}$$

Here $D_{i,\{\alpha,\beta\}}$ is the density matrix corresponding to the Hamiltonian $H0+\Delta H$. We assume that an atomic configuration composed of electrically neutral atoms, i.e. corresponding to electron density $\rho_{\mathrm{ref}}(r)$, is described by a non-SC Hamiltonian $H0$. ΔH accounts for the charge transfer, and its particular diagonal sub-blocks become non-zero when the electron density of corresponding atoms deviates from $\rho^{\mathrm{atom}}_{\mathrm{ref}}$. ΔH is evaluated self-consistently through equations (2) and (3), where $\delta\rho(r)$ is the second term in equation (6).

There are several choices of reference structure because the original EDTB parametrization was chosen to fit simultaneously DFT band structures for linear, graphite, diamond, sc, bcc, and fcc carbon lattices. As already mentioned, $\rho_{\mathrm{ref}}^{\mathrm{atom}}$ is chosen to be fixed rather than environment dependent. That means that the equation $\Delta H = 0$ cannot be satisfied simultaneously for all fitted lattices. Fortunately, if $\rho_{\mathrm{ref}}^{\mathrm{atom}}$ is evaluated for a diamond lattice, ΔH appears to be reasonably small for the other lattices used in the original fitting procedure. Of the periodic structures used to parameterize the EDTB model for carbon, the linear chain gives the largest magnitude of non-physical ΔH. In this case the largest magnitude ΔH element equals 0.16 eV, which results in non-physical spectrum line shifts of less than 0.45 eV. Other periodic lattices have smaller deviations from the reference density, and hence smaller non-physical additions to the Hamiltonian matrix elements. If a moment decomposition is used for the difference between the electron densities of sp and sp^3 hybridized atoms, the lowest-order non-zero moment is a quadrupole. Therefore the resulting additional Coulomb potential does not have a significant effect on the overall system spectrum and charge distribution.

Along with density matrices, which may have non-zero elements if α and β belong to different atoms, uncompensated Mulliken populations (MPs)

$$q_{\alpha\beta} = D_{\alpha,\beta} - D_{\alpha,\beta}^{\mathrm{ref}} \qquad \text{if } \{\alpha,\beta\} \in \text{ Same Atom}, \qquad q_{\alpha\beta} = 0 \text{ otherwise} \tag{7}$$

are used below. Here $D_{\alpha,\beta}^{\mathrm{ref}}$ is the non-SC EDTB density matrix in bulk diamond. For carbon, $D_{s,s}^{\mathrm{ref}} = 1.202\,85$, $D_{px,px}^{\mathrm{ref}} = D_{py,py}^{\mathrm{ref}} = D_{pz,pz}^{\mathrm{ref}} = 0.932\,38$, $D_{\alpha,\beta}^{\mathrm{ref}} = 0$ if $\alpha \neq \beta$. For hydrogen, $D_{s,s}^{\mathrm{ref}} = 1$. The MP matrix has the same block-diagonal structure as ΔH. It contains only those components of the density matrix that contribute to electron density in the block-diagonal approximation. Because the MP matrix is sparse it is convenient to represent it as a vector with ten unique components per carbon atom and one component per hydrogen atom.

The block-diagonal approximation imposed by a convergence acceleration scheme was assumed when evaluating the Hartree and exchange integrals required for ΔH. The Hartree integrals are otherwise evaluated exactly. The exchange integrals are evaluated approximately as a first-order expansion over an equilibrium electron density. A complete form of the SC correction then can be written as ($\{\alpha,\beta\} \in$ Same Atom)

$$\Delta H_{\alpha\beta} = \sum_{\substack{\gamma=1,\delta=1 \\ \{\gamma,\delta\}\in\mathrm{SameAtom}}}^{N} q_{\gamma\delta} \int\int \frac{\varphi_\alpha(r)\varphi_\beta(r)\varphi_\gamma(R)\varphi_\delta(R)}{|r-R|}\,\mathrm{d}R\,\mathrm{d}r + \sum_{\substack{\gamma,\delta \\ \{\alpha,\beta,\gamma,\delta\}\in\mathrm{SameAtom}}} q_{\gamma\delta} \int \varphi_\alpha(r)\varphi_\beta(r)\varphi_\gamma(r)\varphi_\delta(r)[\partial V_{\mathrm{ex}}(\rho)/\partial\rho|_{\rho=\rho_{\mathrm{ref}}}]\,\mathrm{d}r. \tag{2a}$$

Because of the short range nature of the exchange potential, the summation in the last term is performed only over indices that belong to the same atom as indices α and β. The correction due to the external electric field with components E_x, E_y, and E_z is

$$\Delta H_{\alpha\beta}^{\mathrm{external}} = \int \varphi_\alpha(r)[E_x(x-x_0) + E_y(y-y_0) + E_z(z-z_0)]\varphi_\beta(r)\,\mathrm{d}r, \tag{9}$$

where (x_0, y_0, z_0) is the point where the applied potential equals zero.

3.2. Parametrization

A Gaussian basis set is chosen to allow fast analytical evaluation of the Hartree and exchange integrals. The functional forms for carbon and hydrogen atomic orbitals are given by

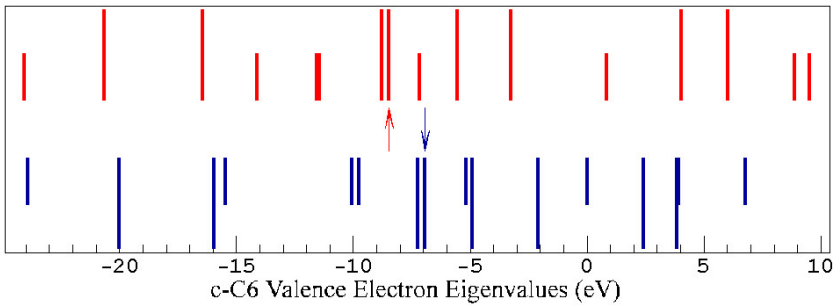

Figure 1. DFT (top) and SC-EDTB (bottom) spectra for cyclic C_6. The line lengths are proportional to the degeneracy of the levels; short lines correspond to non-degenerate levels. The arrows mark HOMO states. The C_6 ring spectrum as well as all other SC-EDTB spectra shown below are shifted by $E_{\text{Shift}} = -5.96$ eV.

equations (10*a*) and (10*b*), respectively:

$$\varphi_s = A_1 \exp(-as_1 r^2) + A_2 \exp(-as_2 r^2)$$
$$\varphi_{p\alpha} = 2ap^{5/4}\left(\frac{2}{\pi}\right)^{3/4} X_\alpha \exp(-apr^2) \qquad (10a)$$

$$\varphi_{\text{H}} = a^{3/4}\left(\frac{2}{\pi}\right)^{3/4} \exp(-ar^2), \qquad (10b)$$

where X_α is either x, y or z. The coefficient A_2 is obtained from the normalization condition, and A_1, as_1, as_2, and ap are chosen to provide the best fit to DFT spectra and charge distributions of cyclic C_6 and a C_5 linear chain[1]. Because the original EDTB method was developed for pure carbon systems, the parameters EH_{OnSite}, SS_σ, and SP_σ used to describe C–H bonds and parameter a for the φ_{H} atomic orbital must be defined. No interaction between electrically neutral hydrogen atoms is assumed.

3.2.1. Carbon orbital parameters. In contrast to DFT, TB schemes usually do not provide the correct *absolute* values for eigenvalue spectra. The correct positioning of the spectrum on an absolute scale is not necessary if only the total energy or forces are desired. Adding the appropriate constant to the TB repulsive term can compensate the constant displacement for each spectrum line. However, the correct absolute position becomes crucial if TB and DFT spectra matching is used to define TB orbital or bond parameters. The first step is to obtain the value of constant shift E_{Shift} to be added to every EDTB spectral line to obtain the best fit to a corresponding DFT spectra. The goal of this parametrization is to obtain the electronic properties of the system rather than total energies. For that reason, matching both occupied and unoccupied levels is emphasized, at least in the vicinity of the Fermi energy. To optimize E_{Shift}, the weighted squared differences between the EDTB and DFT spectra for cyclic C_6 are minimized. The highest weights were assigned for levels lying near the HOMO and LUMO orbitals, lower weights for other occupied levels, and the lowest weights for high unoccupied levels. The resulting value of E_{Shift} is -5.96 eV. Plotted in figure 1 are DFT and SC-EDTB spectra for cyclic C_6, where the latter is shifted by E_{Shift}.

The next step is to find the A_1, as_1, as_2, and ap coefficients for the carbon orbitals (table 1). These parameters were obtained by matching the C_5 linear chain and cyclic C_6 MPs

[1] CERIUS2 4.0 by Molecular Simulations, Inc. was used to compute the DFT electronic structure using the builders: ADF.

Table 1. Optimized carbon orbital parameters. as_1, as_2, and ap are in Å^{-2}. To conserve orbital normalization, high precision is given for these parameters; however, only the two first significant digits have physical meaning. The parameter choice is not unique as the target function is not unique.

A_1	A_2	as_1	as_2	ap
0.082 156 45	0.598 0878	0.112 9953	1.500 468	1.608 523

Table 2. MPs for a C_5 linear chain in external electric fields of different magnitudes. The SC-EDTB values were obtained with the parameters given in table 1.

Field (V Å^{-1})	Method	Atom #1	Atom #2	Atom #3	Atom #4	Atom #5
0.000	SC-EDTB	−0.067	0.231	−0.329	0.231	−0.067
	DFT	−0.001	0.095	−0.188	0.095	−0.001
0.514	SC-EDTB	0.030	0.235	−0.327	0.224	−0.162
	DFT	0.122	0.129	−0.196	0.055	−0.111
1.028	SC-EDTB	0.128	0.236	−0.322	0.215	−0.256
	DFT	0.236	0.146	−0.192	0.024	−0.214
1.542	SC-EDTB	0.227	0.234	−0.314	0.202	−0.348
	DFT	0.353	0.156	−0.185	−0.011	−0.312
2.056	SC-EDTB	0.326	0.229	−0.303	0.187	−0.438
	DFT	0.474	0.159	−0.175	−0.052	−0.405
2.571	SC-EDTB	0.426	0.221	−0.288	0.168	−0.526
	DFT	0.597	0.157	−0.162	−0.098	−0.494

Table 3. Dipole moment and energy decrease for a C_5 linear chain when it is placed in a 2.571 V Å^{-1} external electric field.

	SC-EDTB	DFT	Relative error (%)
Dipole moment	2.51 eÅ	3.60 eÅ	30
Energy decrease	−3.21 eV	−4.56 eV	30

and SC-EDTB spectra lines (shifted by E_{Shift}) to their DFT counterparts. The target function also includes linear C_5 squared atomic MP deviations for various applied fields. The field is directed along the chain and its magnitude has six different values: 0.0, 0.514, 1.028, 1.542, 2.056, and 2.571 V Å^{-1} (table 2). In addition, separate values of MP for s- and p-orbitals for cyclic C_6 are matched. Table 3 compares the response of DFT and SC-EDTB models to the applied electric field for linear C_5.

3.2.2. Hydrogen and C–H bond parameters. To complete the parametrization, the hydrogen orbital coefficient a (10b), and C–H bond parameters EH_{OnSite}, SS_σ, and SP_σ together with their scaling function must be defined. The scaling functions for SS_σ, and SP_σ are taken from the work by Davidson and Pickett [25]. This function reproduces the DFT dependence of occupied eigenlevels versus C–H bond length in methane. At the same time a choice must be made for EH_{OnSite}, SS_σ, and SP_σ because these parameters complement the SC corrections. In addition, the values for EH_{OnSite}, SS_σ, and SP_σ given by Davidson and Pickett lead to the wrong signs for MPs for C–H bonds; carbon appears to be less electronegative than hydrogen.

To optimize a, EH_{OnSite}, SS_σ, and SP_σ, a target function is built that fits MPs and eigenvalue spectra for benzene, methane, and ethane. The target function also includes a

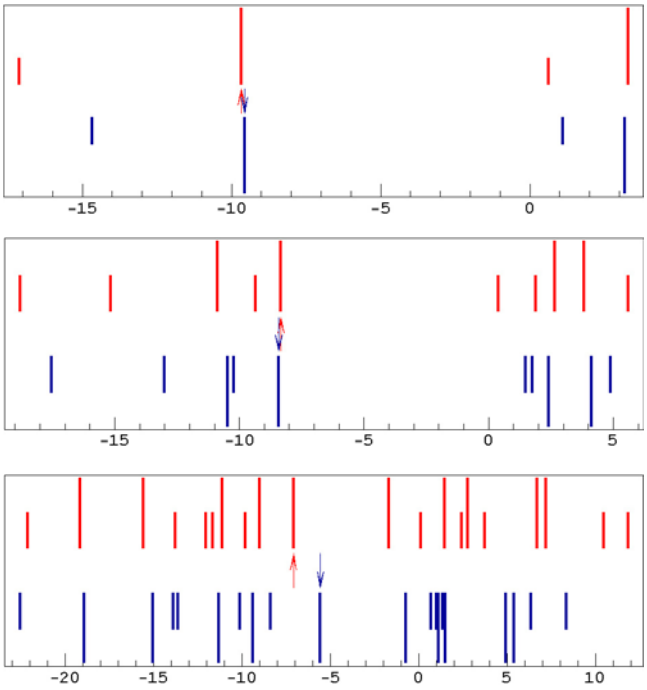

Figure 2. Methane (top), ethane (centre), and benzene (bottom) spectra. The upper portion of each plot shows the DFT spectrum, the lower portion shows the SC-EDTB results.

Table 4. Optimized hydrogen orbital exponential coefficient ($Å^{-2}$), and C–H bond parameters (eV).

a	EH_{OnSite}	SS_σ	SP_σ
2.741 01	3.520 45	−3.331 11	5.492 73

Table 5. MPs for carbon atoms in hydrocarbon molecules.

	Methane		Ethane		Benzene	
	SC-EDTB	DFT	SC-EDTB	DFT	SC-EDTB	DFT
MP s-orbital	0.334	0.266	0.240	0.252	0.083	0.167
MP p-orbital	0.507	0.815	0.328	0.592	0.121	0.140
MP Total	0.840	1.081	0.568	0.844	0.203	0.307

subfunction for fitting MPs in a small hydrogen-passivated diamond cluster with {111} and {100} facets[2]. Spectra moments fitting for benzene and eigenlevel fitting for methane and ethane is performed. The optimized values of a, EH_{OnSite}, SS_σ, and SP_σ are given in table 4. Table 5 compares MPs for hydrocarbon molecules obtained from SC-EDTB and DFT simulations. The values from tables 1 and 4 were used to obtain molecular (figure 2) and hydrogen-passivated diamond clusters spectra (figure 3). The electron affinity value for the hydrogenated nano-diamond particle can be read directly from the energy spectrum

[2] CERIUS2 4.0 by Molecular Simulations, Inc. was used to compute the DFT electronic structure using the builders: DMOL3.

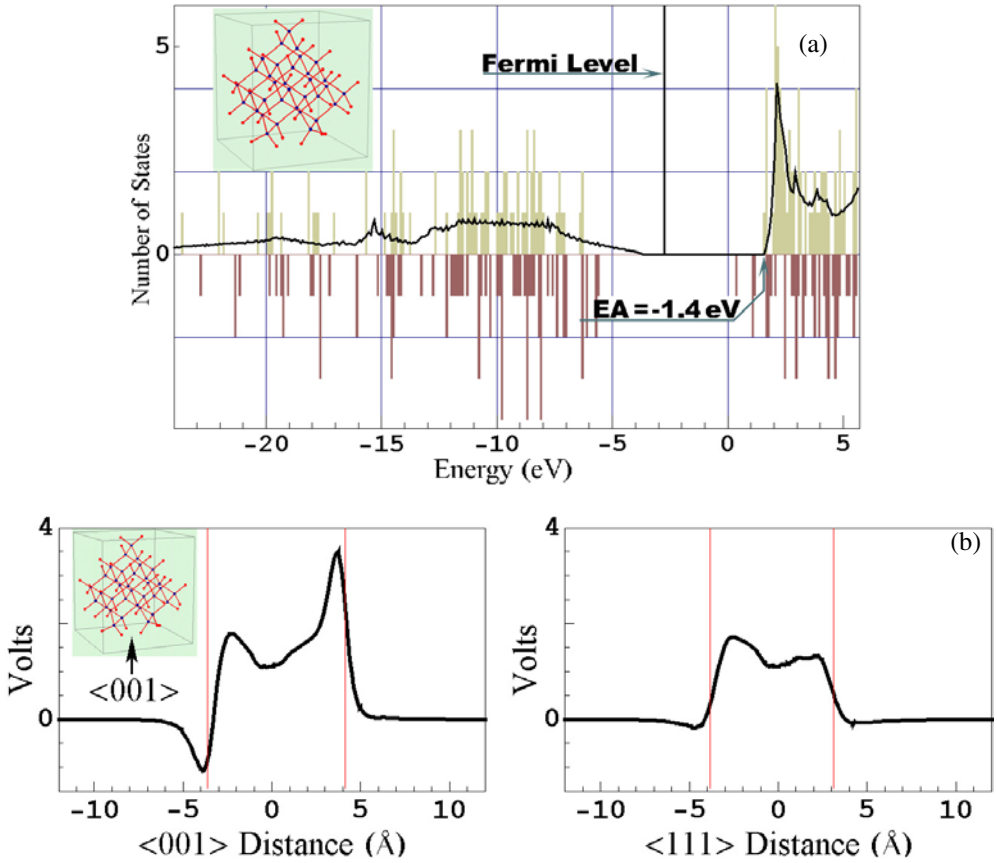

Figure 3. Properties of a hydrogen-passivated diamond cluster (inset) composed of 34 carbon atoms. (a) SC-EDTB (top) and DF (bottom) spectra. In addition to E_{Shift} the bulk spectrum (solid line) was shifted by 1.6 V average Coulomb potential experienced by carbon atoms in the cluster (cf figure 3(b)). Note that the DF underestimates the bandgap for bulk diamond by approximately 1.0 eV. (b) Coulomb potential profile along ⟨001⟩ and ⟨111⟩ lines passing through the centre of mass of the cluster. The vertical lines mark cluster facets.

plot in figure 3. Experimental [26], SC-EDTB, and DFT [27] electron affinities for a {111} hydrogenated surface are −1.27, −1.4, and −2.03 eV, respectively. The plot in figure 3(a) and all potential plots below depict the Coulomb potential associated with the difference $\rho(r) - \rho_{\text{ref}}(r)$ given by the second term in equation (6) rather than with the total electron density $\rho(r)$. Subtraction of $\rho_{\text{ref}}(r)$ eliminates short-range potential oscillations produced by single atoms and makes the long-range potential component clearly visible.

4. NEGF and convergence acceleration scheme

The NEGF formalism allows one to compute the density matrix for finite-size systems that are connected to semi-infinite periodic leads under an arbitrary bias [2]. For simplicity we assume that the two leads ('left' and 'right') of the same type are connected to the system. They have the same Fermi level μ_0 if no external bias is applied. The left lead is externally biased by

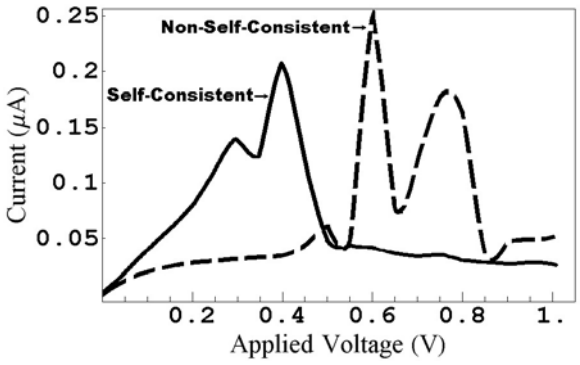

Figure 4. I–V curves. The solid curve corresponds to the SC Hamiltonian $H = H0 + \Delta H$, and the dashed curve to the non-SC Hamiltonian $H = H0$.

$+\Delta V_{\mathrm{L}}$; the right lead by $-\Delta V_{\mathrm{R}}$. The retarded Green function matrix $G(\varepsilon)$ is

$$G_{\alpha,\beta}(\varepsilon) = (\{[\varepsilon + \mathrm{i}\eta]I - [H + \Sigma_{\mathrm{L}}(\varepsilon - \Delta V_{\mathrm{L}}) + \Sigma_{\mathrm{R}}(\varepsilon + \Delta V_{\mathrm{R}})]\}^{-1})_{\alpha,\beta}. \tag{11}$$

Here $\Sigma_{\mathrm{L(R)}}$ is the self-energy of the left (right) lead, I is the identity matrix, and $H = H0 + \Delta H$ is the Hamiltonian of the system. The density matrix D is obtained through integration over ε:

$$D_{\alpha,\beta} = -\frac{2}{\pi}\left\{\int_{-\infty}^{\infty} f(\varepsilon - \Delta V_{\mathrm{L}})G(\varepsilon)\cdot \mathrm{Im}[\Sigma_{\mathrm{L}}(\varepsilon - \Delta V_{\mathrm{L}})]\cdot G^{*}(\varepsilon)\,\mathrm{d}\varepsilon\right\}_{\alpha,\beta}$$
$$-\frac{2}{\pi}\left\{\int_{-\infty}^{\infty} f(\varepsilon + \Delta V_{\mathrm{R}})G(\varepsilon)\cdot \mathrm{Im}[\Sigma_{\mathrm{R}}(\varepsilon + \Delta V_{\mathrm{R}})]\cdot G^{*}(\varepsilon)\,\mathrm{d}\varepsilon\right\}_{\alpha,\beta}. \tag{12}$$

Here f denotes the Fermi function. To facilitate numerical computation most of the integration in (12) is performed in the upper complex half-plane [1]. The concept of the Newton–Raphson algorithm, however, does not depend on the shape of the integration contour. For clarity we assume that equation (12) is used for the evaluation of the density matrix.

The block-diagonal matrix ΔH can be viewed as a double-indexed vector, in the same fashion as MP. If approximation (2a) is used, ΔH is a linear function of input MPs q_{In}. U denotes the matrix of coefficients, which relate ΔH and MP: $\Delta H = U \cdot q_{\mathrm{In}}$. Suppose that δq_{In} is a variation of q_{In}. The variation of output MPs is obtained by differentiation of equations (11) and (12). For example, the first-order variation of the first term integrand in equation (12) is

$$\delta\{G(\varepsilon)\cdot \mathrm{Im}[\Sigma_{\mathrm{L}}(\varepsilon - \Delta V_{\mathrm{L}})]\cdot G^{*}(\varepsilon)\} = G(\varepsilon)\cdot \delta H \cdot G(\varepsilon)\cdot \mathrm{Im}[\Sigma_{\mathrm{L}}(\varepsilon - \Delta V_{\mathrm{L}})]\cdot G^{*}(\varepsilon)$$
$$+ G(\varepsilon)\cdot \mathrm{Im}[\Sigma_{\mathrm{L}}(\varepsilon - \Delta V_{\mathrm{L}})]\cdot G^{*}(\varepsilon)\cdot \delta H \cdot G^{*}(\varepsilon), \tag{13}$$

where δH is a block-diagonal square matrix. Taking into account the linear relationship between δH and δq_{In}, we obtain

$$\delta q_{\mathrm{Out}} = A \cdot \delta q_{\mathrm{In}}. \tag{14}$$

The complete expression for matrix A is too long to be presented here, but its computation is straightforward. The cost of computation of A is $\mathrm{O}(M^2)$ per sampling point. Here M is the length of the MP vector. Given equation (14), the self-consistency condition can be expressed as

$$q_{\mathrm{Out}} + A \cdot \delta q_{\mathrm{In}} = q_{\mathrm{In}} + \delta q_{\mathrm{In}}. \tag{15}$$

Here q_{In} and q_{Out} are known vectors denoting input and output MPs, respectively, in the current SC iteration. Equation (15) is solved for δq_{In} during each iteration. The next iteration input

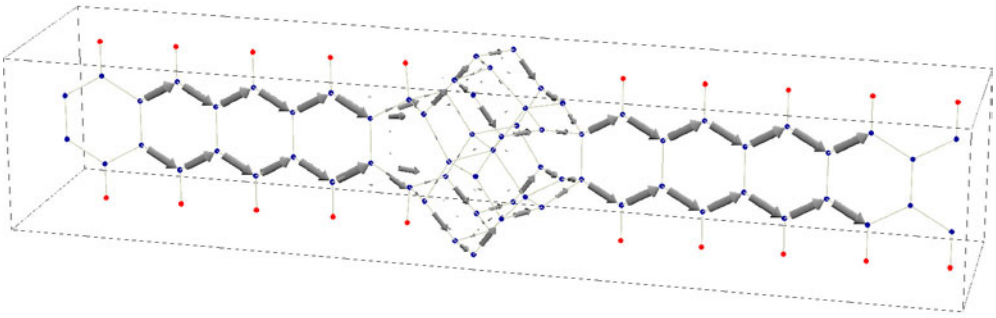

Figure 5. Current density in the polyacene–nano-diamond structure under a 1.0 V external bias. The maximum arrow size corresponds to 0.014 μA.

density is taken as $q_{\mathrm{In}}+\delta q_{\mathrm{In}}$. Solving the linear system (15) for δq_{In} requires $\mathrm{O}(M^3)$ operations. Therefore the total cost of the Newton–Raphson algorithm is $\mathrm{O}(M^3)+N_{\mathrm{SP}}\mathrm{O}(M^2)$ per iteration; N_{SP} is the number of sampling points on the integration contour.

5. Case study: resonant tunnelling device

We consider the structure shown in figures 5–8, which is composed of a 29-atom nano-diamond particle connected to two semi-infinite polyacene leads. Five unit cells for each lead are also considered as part of the system. That brings the total number of atoms in the system to 89. The unpassivated nano-diamond particle is metastable, and reconstructs to an onion-like fullerene structure if complete relaxation is allowed. The unreconstructed particle has a very small HOMO–LUMO gap, and its metallic behaviour originates from the surface states. Although artificial, this system is a good demonstration of a non-equilibrium voltage drop in a completely metallic system.

The total number of orbitals N equals 296 and the size M of derivative matrix A equals 710. Energy integration was performed along the contour similar to the contour shown in [1]. The number of integration points, however, was much greater than in [1]. A large number of sampling points, most of which lie on the real axis portion of the contour, is crucial for a correct density evaluation. A minimal basis set and efficient SC convergence procedure allows more than 600 integration points in the current example.

The current between orbitals α and β is evaluated as [3]

$$J_{\alpha,\beta} = -\frac{2e^2}{\hbar}\,\mathrm{Im}(D_{\alpha,\beta})H_{\alpha,\beta}, \tag{16}$$

where $H = H0 + \Delta H$ is a self-consistent Hamiltonian, and D is a non-equilibrium density matrix obtained through equation (12). Plotted in figure 4 are I–V curves for SC and non-SC Hamiltonians. Figure 4 serves as a demonstration of how important self-consistency can be for non-equilibrium simulations dealing with metallic systems. Figure 5 illustrates the current density for a non-resonant applied bias $\Delta V_{\mathrm{L}} + \Delta V_{\mathrm{R}} = 1.0$ V. The interatomic current is depicted by arrows; the maximum size arrow corresponds to 0.014 μA. Figure 6, which is zoomed-out portion of figure 5, shows that under non-resonant bias the nano-diamond particle conducts through its surface states. Figure 7 illustrates the current density under a resonant bias $\Delta V_{\mathrm{L}} + \Delta V_{\mathrm{R}} = 0.41$ V. The scaling in figure 7 differs from figures 5, 6: the

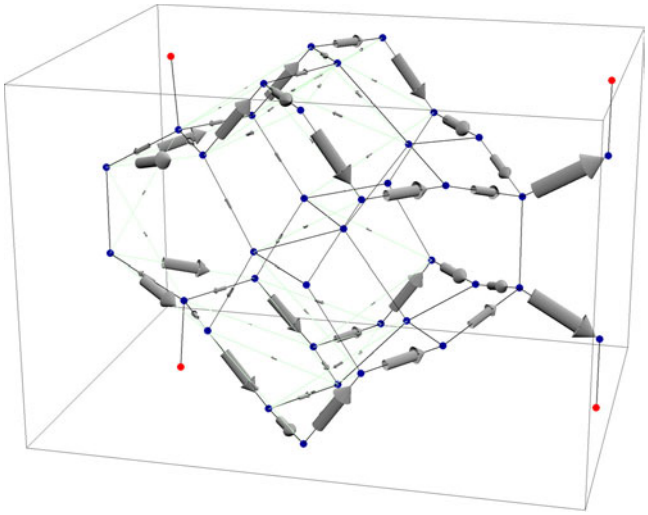

Figure 6. Zoomed-out portion of figure 5. Under non-resonant conditions the cluster conducts through the surface states.

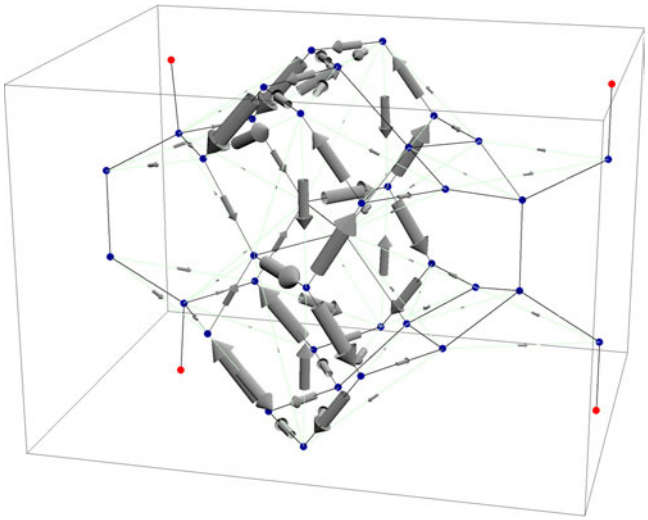

Figure 7. Current density in the polyacene–nano-diamond structure under resonant conditions. The external bias equals 0.41 V. The maximum arrow size corresponds to 0.31 μA.

maximum size arrow corresponds to 0.31 μA. Under resonant bias the nano-particle acts like a resonant cavity. The current density inside the cavity substantially exceeds the current density in the leads. Figures 8, 9 illustrate the Coulomb potential distribution associated with the $\rho(r) - \rho_{\mathrm{ref}}(r)$. Marginal regions depict the Coulomb potential associated with perfect leads and shifted by either ΔV_{L} or by $-\Delta V_{\mathrm{R}}$. A small potential discontinuity can be seen at the right system boundary. It is due to the finite system size. When the system size increases through incorporation of longer lead segments, the potential step disappears.

The polyacene conductivity comes from π-bonding states. Occupied and unoccupied π-dispersion curves touch each other at the Brillouin zone boundary. Under a negligibly small applied bias, conductivity originates from the largest k-vector state $k_{\mathrm{max}} \cong 1.35\ \mathrm{\AA}^{-1}$ (figure 10).

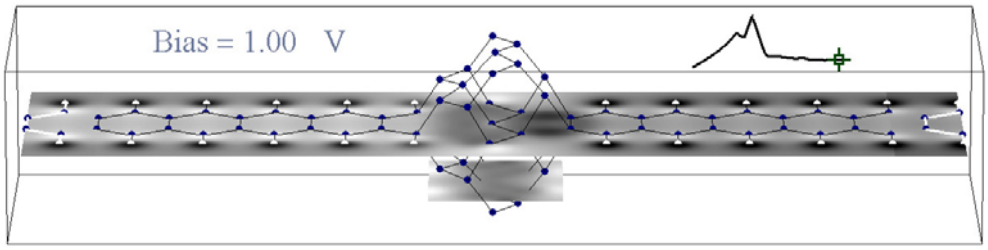

Figure 8. Coulomb potential distribution under 1.0 V external bias.

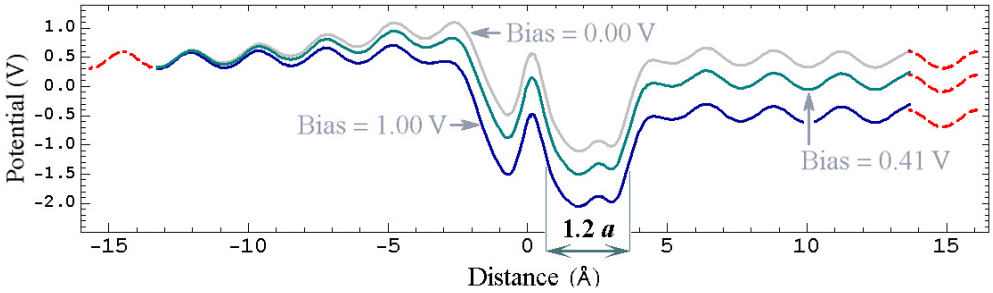

Figure 9. Coulomb potential along the x-axis, which coincides with the polyacene symmetry axis.

$k_{\max}$ corresponds to a half-wavelength equal to the longitudinal size a of the polyacene unit cell. As the applied bias is being increased, states with shorter k-vectors can participate in the conduction. The resonant bias voltage (0.41 V) corresponds to the $\{1.12, 1.35\}$ Å^{-1} range of k-states participating in conduction (cf figure 10). The half-wavelength of these states lies in the range $\{a, 1.2\ a\}$. On the other hand, the 'gap' between the two polyacene leads is 1.68 a (cf figure 7), which means that the resonance condition for the entire cluster is not met. As follows from figures 8, 9, the potential inside the nano-particle has a complex internal structure. It is reasonable to assume that the resonant condition is met with respect to a certain potential feature inside the nano-particle, rather than the nano-particle as a whole. Figure 9 illustrates one of such possibilities. At the same time the complexity of the current pattern and potential profile shows that quantitative resonant conditions can neither be determined from device geometry nor from an equilibrium potential distribution.

6. Conclusions

The non-self-consistent EDTB for carbon was extended to a self-consistent DF-like scheme. Extra parameters required for the SC correction and for C–H bonds were determined by matching MPs and SC-EDTB spectra to their DFT analogues. To illustrate SC-EDTB capabilities, a resonant tunnelling device was considered. The calculations indicate a pronounced resonant effect and negative slope region in the I–V curve.

The accuracy of the method is comparable to the overall accuracy achieved by means of NEGF techniques. Because most NEGF techniques are not exact, there may be no compelling reason for using an *ab initio* scheme with a precision that supersedes the overall quality of the method used to evaluate the electron current. Therefore the SC-EDTB method is a reasonable trade-off between fast but non-self-consistent tight binding, and sometimes unnecessarily precise and computationally expensive DFT calculations. Orthogonal atomic orbitals are

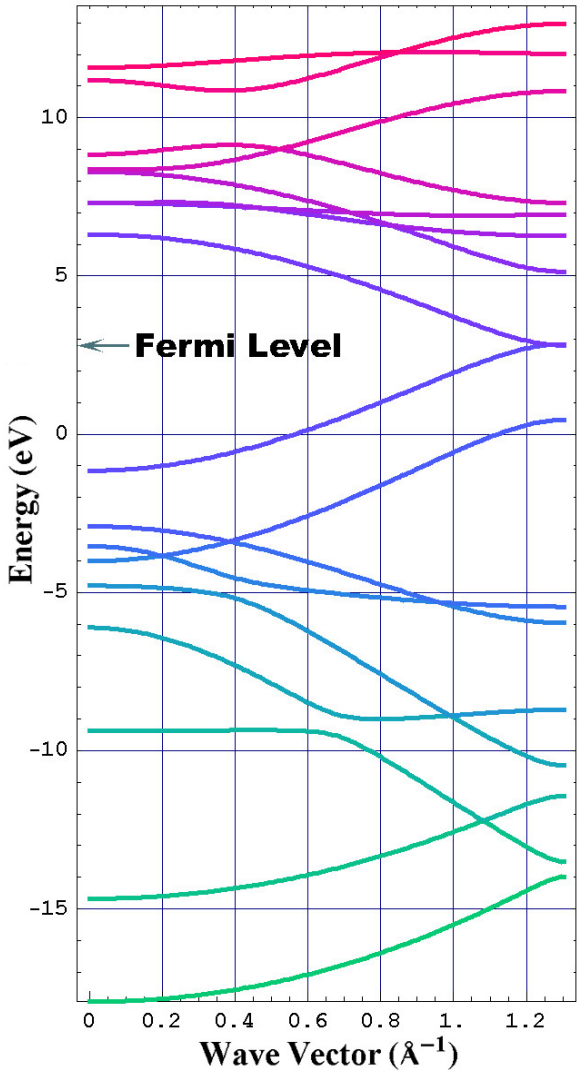

Figure 10. Polyacene SC-EDTB dispersion curves. The energy scale is shifted upwards by 5.96 eV.

assumed so that a Newton–Raphson algorithm for nonlinear systems of equations can be efficiently used to achieve self-consistency. Finally, we believe that employing an environment dependence for atomic orbitals and the atomic density matrix $D^{\mathrm{ref}}_{\alpha,\beta}$ can substantially enhance the precision of SC-EDTB.

Acknowledgments

Helpful discussions with A Buldum, M Buongiorno-Nardelli, J-P Lu, J Mintmire, O Zhou, J Bernholc, and P P Schmidt are gratefully acknowledged. This work was supported by a Multi-University Research Initiative funded by the Office of Naval Research through a subcontract from the University of North Carolina at Chapel Hill. The work has been completed at Naval Research Laboratory, Code 6180.

References

[1] Brandbyge M, Mozos J L, Ordejon P, Taylor J and Stokbro K 2002 Density-functional method for nonequilibrium electron transport *Phys. Rev.* B **65** 165401
[2] Datta S 2000 Nanoscale device modeling: the Green's function method *Superlatt. Microstruct.* **28** 253
[3] Todorov T N 2002 Tight-binding simulation of current carrying nanostructures *J. Phys.: Condens. Matter* **14** 3049
[4] Roland C, Nardelli M B, Wang J and Guo H 2000 Dynamic conductance of carbon nanotubes *Phys. Rev. Lett.* **84** 2921
[5] Bernholc J *et al* 2000 Large-scale applications of real-space multigrid methods to surfaces, nanotubes, and quantum transport *Phys. Status Solidi* b **217** 685
[6] Derosa P A and Seminario J M 2000 Electron transport through single molecules: scattering treatment using density functional and Green function theories *J. Chem. Phys.* **105** 471
[7] Damle P, Ghosh A W and Datta S 2002 First-principles analysis of molecular conduction using quantum chemistry software *Chem. Phys.* **281** 171
[8] Aviram A and Ratner M (ed) 1998 *Ann. New York Acad. Sci.* (Special issue on Molecular Electronics: Science and Technology)
[9] Areshkin D A, Shenderova O A, Schall J D and Brenner D W 2003 Convergence acceleration scheme for self-consistent orthogonal-basis-set electronic structure methods *Mol. Simul.* **29** 269
[10] Broyden C G 1965 A class of methods for solving nonlinear simultaneous equations *Math. Comput.* **19** 577
[11] Pulay P 1982 Improved SCF convergence acceleration *J. Comput. Chem.* **3** 556
[12] Tang M S, Wang C Z, Chan C T and Ho K M 1996 *Phys. Rev.* B **53** 979
Tang M S, Wang C Z, Chan C T and Ho K M 1996 *Phys. Rev.* B **54** 10982
[13] For a review, see Goringe C M, Bowler D R and Hernandez E 1997 *Rep. Prog. Phys.* **60** 1447
[14] Xu C H, Wang C Z, Chan C T and Ho K M 1992 *J. Phys.: Condens. Matter* **4** 6047
[15] Sankey O F and Niklewski D J 1989 *Phys. Rev.* B **40** 3979
[16] Porezag D, Frauenheim Th, Köhler Th, Seifert G and Kaschner R 1995 *Phys. Rev.* B **51** 12947
[17] Elstner M, Porezag D, Jungnickel G, Elsner J, Haugk M, Frauenheim T, Suhai S and Seifert G 1998 *Phys. Rev.* B **58** 7260
[18] Frauenheim T, Seifert G, Elstner M, Hajnal Z, Jungnickel G, Porezag D, Suhai S and Scholz R 2000 *Phys. Status Solidi* b **217** 41
[19] Sternberg M, Galli G and Frauenheim T 1999 *Comput. Phys. Commun.* **118** 200
[20] Tsai M-H, Sankey O F and Dow D 1992 *Phys. Rev.* B **46** 10464
[21] Halley J W, Michalewicz M T and Tit N 1990 *Phys. Rev.* B **41** 10165
[22] Yu N and Halley J W 1995 *Phys. Rev.* B **51** 4768
[23] Zhuang M and Halley J W 2001 *Phys. Rev.* B **64** 024413
[24] Esfarjani K and Kawazoe Y 1998 *J. Phys.: Condens. Matter* **10** 8257
[25] Davidson B N and Pickett W E 1994 *Phys. Rev.* B **49** 11253
[26] Ristein J 2000 *Diamond Relat. Mater.* **9** 1129
[27] Rutter M J and Robertson J 1998 *Phys. Rev.* B **57** 9241